

Device simulation of quasi-two-dimensional perovskite/silicon tandem solar cells towards 30%-efficiency

Xiao-Ping Xie(谢小平), Qian-Yu Bai(白倩玉), Gang Liu(刘刚), Peng Dong(董鹏), Da-Wei Liu(刘大伟), Yu-Feng Ni(倪玉凤), Chen-Bo Liu(刘晨波), He Xi(习鹤), Wei-Dong Zhu(朱卫东), Da-Zheng Chen(陈大正), and Chun-Fu Zhang(张春福)

Citation: Chin. Phys. B, 2022, 31 (**10**): 108801. DOI: 10.1088/1674-1056/ac7292
Journal homepage: http://cpb.iphy.ac.cn; http://iopscience.iop.org/cpb

What follows is a list of articles you may be interested in

Reveal the large open-circuit voltage deficit of all-inorganicCsPbIBr$_2$ perovskite solar cells

Ying Hu(胡颖), Jiaping Wang(王家平), Peng Zhao(赵鹏), Zhenhua Lin(林珍华), Siyu Zhang(张思玉), Jie Su(苏杰), Miao Zhang(张苗), Jincheng Zhang(张进成), Jingjing Chang(常晶晶), and Yue Hao(郝跃)

Chin. Phys. B, 2022, 31 (**3**): 038804. DOI: 10.1088/1674-1056/ac464b

Effect of carrier mobility on performance of perovskite solar cells

Yi-Fan Gu(顾一帆), Hui-Jing Du(杜会静), Nan-Nan Li(李楠楠), Lei Yang(杨蕾), Chun-Yu Zhou(周春宇)

Chin. Phys. B, 2019, 28 (**4**): 048802. DOI: 10.1088/1674-1056/28/4/048802

Efficient design of perovskite solar cell using mixed halide and copper oxide

Navneet kour, Rajesh Mehra, Chandni

Chin. Phys. B, 2018, 27 (**1**): 018801. DOI: 10.1088/1674-1056/27/1/018801

Simulation design of P-I-N-type all-perovskite solar cells with high efficiency

Hui-Jing Du(杜会静), Wei-Chao Wang(王韦超), Yi-Fan Gu(顾一帆)

Chin. Phys. B, 2017, 26 (**2**): 028803. DOI: 10.1088/1674-1056/26/2/028803

Device simulation of lead-free $CH_3NH_3SnI_3$ perovskite solar cells with high efficiency

Hui-Jing Du(杜会静), Wei-Chao Wang(王韦超), Jian-Zhuo Zhu(朱键卓)

Chin. Phys. B, 2016, 25 (**10**): 108802. DOI: 10.1088/1674-1056/25/10/108802

Device simulation of quasi-two-dimensional perovskite/silicon tandem solar cells towards 30%-efficiency

Xiao-Ping Xie(谢小平)[1,†], Qian-Yu Bai(白倩玉)[2,†], Gang Liu(刘刚)[1], Peng Dong(董鹏)[1], Da-Wei Liu(刘大伟)[1], Yu-Feng Ni(倪玉凤)[1], Chen-Bo Liu(刘晨波)[2], He Xi(习鹤)[2], Wei-Dong Zhu(朱卫东)[2], Da-Zheng Chen(陈大正)[2,‡], and Chun-Fu Zhang(张春福)[2]

[1] *Qinghai Huanghe Hydropower Development CO., LTD., Xining* 810008, *China*

[2] *State Key Discipline Laboratory of Wide Band Gap Semiconductor Technology, Xidian University, Xi'an* 710071, *China*

(Received 2 March 2022; revised manuscript received 10 May 2022; accepted manuscript online 24 May 2022)

Perovskite/silicon (Si) tandem solar cells have been recognized as the next-generation photovoltaic technology with efficiency over 30% and low cost. However, the intrinsic instability of traditional three-dimensional (3D) hybrid perovskite seriously hinders the lifetimes of tandem devices. In this work, the quasi-two-dimensional (2D) $(BA)_2(MA)_{n-1}Pb_nI_{3n+1}$ ($n = 1, 2, 3, 4, 5$) (where MA denotes methylammonium and BA represents butylammonium), with senior stability and wider bandgap, are first used as an absorber of semitransparent top perovskite solar cells (PSCs) to construct a four-terminal (4T) tandem devices with a bottom Si-heterojunction cell. The device model is established by Silvaco Atlas based on experimental parameters. Simulation results show that in the optimized tandem device, the top cell ($n = 4$) obtains a power conversion efficiency (PCE) of 17.39% and the Si bottom cell shows a PCE of 11.44%, thus an overall PCE of 28.83%. Furthermore, by introducing a 90-nm lithium fluoride (LiF) anti-reflection layer to reduce the surface reflection loss, the current density (J_{sc}) of the top cell is enhanced from 15.56 mA/cm^2 to 17.09 mA/cm^2, the corresponding PCE reaches 19.05%, and the tandem PCE increases to 30.58%. Simultaneously, in the cases of $n = 3$, 4, and 5, all the tandem PCEs exceed the limiting theoretical efficiency of Si cells. Therefore, the 4T quasi-2D perovskite/Si devices provide a more cost-effective tandem strategy and long-term stability solutions.

Keywords: two-dimensional, device simulation, antireflection layers, tandem solar cells

PACS: 88.40.H–, 88.40.J–, 88.40.hj **DOI:** 10.1088/1674-1056/ac7292

1. Introduction

Silicon (Si) solar cells have dominated the photovoltaic market so far due to their high performance and high reliability since their advent in 1954.[1] Now their power conversion efficiency (PCE) has reached 26.67%,[2] which is approaching their maximum theoretical PCE of 29.4%.[3] To break through this efficiency bottleneck at a lower cost, a tandem technology of metal halide perovskite top cells and crystalline Si bottom cells has attracted explosively increasing attention in both academia and industry areas.[4,5] This is due to the perovskite solar cells (PSC) possessing the advantages of tunable bandgap, bipolar transport, high carrier mobility, easy fabrication process, low cost, and the rapidly increased PCE from 3.8% to 25.7% during ten years.[6–10] Also the theoretical PCE of perovskite/Si tandem cells is as high as 43%,[11] what is more exciting is that they have achieved a laboratory PCE of 29.80% (certified), an efficiency over the theoretical limit of Si cells.

Perovskite/Si tandem solar cells mainly include two structures of two-terminal (2T, monolithic) and four-terminal (4T, mechanically stacked) devices.[12,13] Comparing with the 2T devices, the main issue of current matching does not exist in 4T devices, where the top perovskite cell and bottom Si cell can be fabricated separately and optimized individually, presenting the natural process compatibility. Nowadays, a PCE of 28.3% has been reported in 4T-perovskite/Si devices,[14] which is also very close to the theoretical limit of Si cells. More importantly, owing to the intrinsic instability of perovskite under light, heat, and moisture conditions induced by the organic cation (MA^+ or FA^+) components,[15] the lifetime of organic–inorganic hybrid perovskite devices (several years) is shorter than that of Si cells (> 20 years), which will significantly shorten the operating life of 2T-perovskite/Si tandem devices. While in the 4T tandem modules, the degraded top cells can be replaced easily by new PSCs and the bottom Si modules keep working, which provides another route to improving the longtime stability of perovskite/Si tandem devices in practical applications.

To further improve the stability of perovskite material, it has been proved to be effective to substitute MA^+ or FA^+ by inorganic cation (Cs^+), however, the relatively wide bandgap of more stable $CsPbIBr_2$ (~ 2.0 eV)[16] or $CsPbBr_3$ (~ 2.3 eV)[17] limits the ability to absorb light and the PCE of corresponding PSCs; the high crystal temperature (over

[†]These authors contributed equally to this study.

[‡]Corresponding author. E-mail: dzchen@xidian.edu.cn

© 2022 Chinese Physical Society and IOP Publishing Ltd

200 °C)[18] is also not expected for the cost-effective PSCs. Fortunately, the emerging quasi-2D perovskite materials have been considered as one of the most promising strategies to address the instability problem, and found wide applications in light-emitting diodes, photodetectors, and solar cells.[19,20] The quasi-2D perovskite was obtained by cutting off a piece of traditional 3D perovskite along its crystallographic plane and inserting big organic cations to separate the inorganic parts, which behaves like multilayer quantum wells and exhibits greatly improved air, phase, and thermal stability.[21] Simultaneously, the PCE of quasi-2D PSCs increased steadily and exceeded 20%[22,23] by orientation adjustment, organic-spacer-cations design, composition engineering, and device engineering.[21]

The most studied Ruddlesden–Popper (RP) 2D perovskite showed a structure of $(R\mathrm{NH_3})_2\mathrm{A}_{n-1}\mathrm{M}_n\mathrm{X}_{3n+1}$, where R represents an aliphatic alkylammonium or aromatic cation, n denotes the 'quantum-well' thickness or the layer number of perovskite sheets.[24] Particularly, both the n and organic components can be used to modulate the bandgap, absorbance, and exciton binding energy of 2D perovskite material. In 2016, the successful fabrication of vertically oriented $(\mathrm{BA})_2(\mathrm{MA})_3\mathrm{Pb}_4\mathrm{I}_{13}$ by hot-casting[19] paved the way to develop RP 2D-PSCs, and now the PCE over 18% has been reported.[25–27] Song *et al.* performed a systematic spectroscopic ellipsometry study and extracted the optical dielectric functions and complex refractive indices of phase-pure RP and DJ phase perovskite, which opens the door for modeling and simulating 2D perovskite-based optoelectronic devices.[28]

In this work, the semitransparent quasi-2D PSCs with an absorber of $(\mathrm{BA})_2(\mathrm{MA})_{n-1}\mathrm{Pb}_n\mathrm{I}_{3n+1}$ ($n = 1, 2, 3, 4, 5$) is used as a top cell to construct a 4T-tandem solar cell with an Si-heterojunction bottom cell. The tandem device model has been established by Silvaco Atlas based on the experimental parameters, and the photovoltaic performances for quasi-2D perovskite/Si PSCs have been studied systematically. Simulation results for single-junction PSCs show that the device presents a senior PCE of 17.64% when the n value is chosen as 4, which is consistent with the experimental report. In the 4T-tandem device, the top cell ($n = 4$) obtains a PCE of 17.39% and the filtered Si bottom cell possesses a PCE of 11.44%, thus an overall PCE arrives at 28.83%. Furthermore, when a 90-nm LiF anti-reflection layer is introduced, the J_{sc} of the top cell is enhanced from 15.56 mA/cm^2 to 17.09 mA/cm^2, *i.e.*, the increment is 9%, the corresponding PCE reaches 19.05% and the overall PCE of the tandem device rises to 30.58%. Simultaneously, in the case of $n = 3$, $n = 4$, and $n = 5$, all the tandem PCE exceeds 30%, which is greater than the limiting theoretical efficiency of silicon cells. Therefore, besides the improved long-term stability, the 4T quasi-2D perovskite/Si devices provide a more cost-effective tandem strategy to break through the theoretical efficiency limit of Si cells and hold their dominance in the PV market.

2. Theory and methods

Silvaco TCAD Atlas device simulator is used to establish the model of single-junction quasi-2D RP PSCs and 4T-perovskite/Si-heterojunction tandem based on the optical and electrical parameters (see Tables S1 and S2 in supporting information) in experimental reports.[29–37] In addition, because the carrier dynamics of quasi-2D perovskite films are closely related to the n value, the mobility, carrier concentration and effective state density are inconsistent with different n values. Taking the perovskite film with $n = 4$ as a reference, the perovskite model with different mobilities, doping carrier concentration, and effective state density is analyzed and calculated. Figure S1 in supporting information shows the relationship between the electrical performance and mobility of the device. It can be seen that the change in mobility has no great influence on the electrical performance of the device. Table S3 shows the relationship between the electrical properties of the device and the carrier concentration. When the carrier concentration (N_{D}) changes, the electrical properties of the device do not change significantly. From Table S4, with the increase of the state density (N_{C} and N_{V}), only the open-circuit voltage (V_{oc}) of device changes within the theoretical range[34,38,39] and other parameters are basically unchanged. Therefore, since the electron mobility (M_{un}), hole mobility (M_{up}), N_{D}, N_{C}, and N_{V} have little influence on the overall calculation, $n = 1$, 2, 3, 4, and 5 are calculated on the basis of $M_{\mathrm{un}} = M_{\mathrm{up}} = 50$, $N_{\mathrm{D}} = 1 \times 10^{13}$, and $N_{\mathrm{C}} = N_{\mathrm{V}} = 1 \times 10^{20}$. The device geometry as well as the structure of quasi-2D $(\mathrm{BA})_2(\mathrm{MA})_{n-1}\mathrm{Pb}_n\mathrm{I}_{3n+1}$ perovskite when $n = 1$, $n = 2$, $n = 3$, $n = 4$, and $n = 5$ is shown in Fig. 1. Here, it is assumed that the quantum-well structured quasi-2D perovskite has homogeneous energy landscape and shows no cascade energy transfer behaviors. The top cell possesses a structure of ITO/$\mathrm{SnO_2}$/quasi-2D perovskites/spiro-OMeTAD/ITO, the LiF acts as an anti-reflection layer, and the parameters of Si-heterojunction cells are identical to those in our previous research.[40] In addition, a refractive matching layer[41] with a refractive index of about 1.414 is used between the top cell and the bottom cell to reduce the light loss at the interface between the sub-cells. Then the light absorption, J–V characteristics, and optical electric field distributions are systemically studied to obtain an optimal tandem device structure and understand the photoelectric conversion mechanism. The simulations are mainly based on three basic equations, *i.e.* Poisson's equation, carrier continuity equation, and drift-diffusion equation,[42] and the detailed calculation method can be found in our previous researches.[40,43,44]

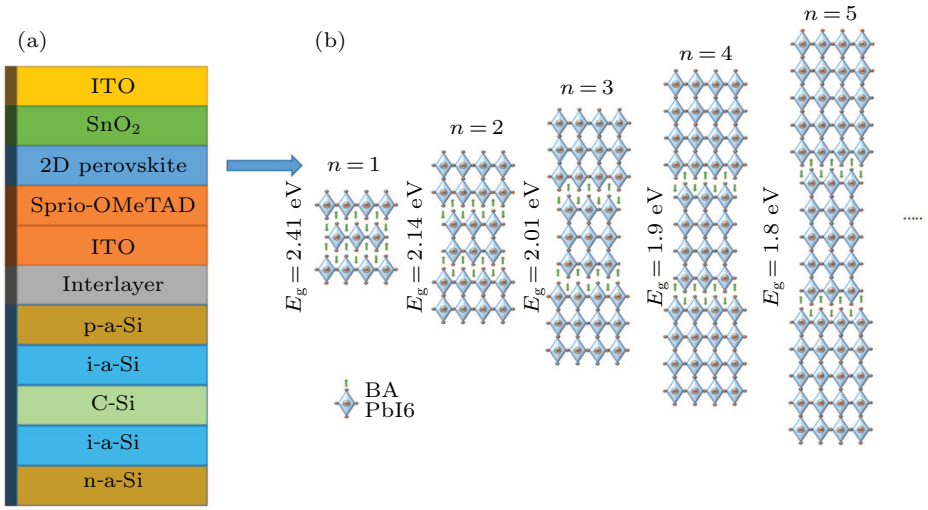
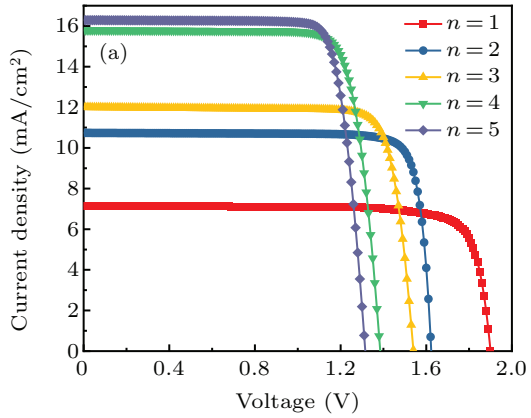


Fig. 1. (a) The 4T-tandem solar cell structure and (b) schematic crystal structure of quasi-2D RP $(BA)_2(MA)_{n-1}Pb_nI_{3n+1}$ perovskites with various values of n and bandgap.

3. Results and discussion

Comparing the conventional 3D perovskites, the remarkably enhanced stability against moisture of the 2D perovskites can be attributed to the Van der Waals interactions between the organic spacer cations. The lower the value of n, the higher the stability for 2D perovskite is.[45] It has been verified that the 2D perovskite with $n = 1$ immersing in water can be maintained several minutes without any decomposition from perovskite to lead iodide.[46] On the other hand, the bandgap of 2D perovskites increases with the decreasing of n value, and the wider bandgap will limit their light absorption range and the PCE of PSCs.



(b)

2D PSCs	J_{sc} (mA/cm²)	V_{oc} (V)	*FF* (%)	*PCE* (%)
$n = 1$	7.18	1.90	81.55	11.12
$n = 2$	10.89	1.62	81.72	14.63
$n = 3$	12.01	1.54	82.90	15.34
$n = 4$	15.81	1.39	80.56	17.63
$n = 5$	16.32	1.32	81.73	17.53

Fig. 2. (a) Calculated *J*–*V* curves and (b) photovoltaic parameters of single junction quasi-2D $(BA)_2(MA)_{n-1}Pb_nI_{3n+1}$ PSCs with varying n values.

Consequently, the cases of $n \leq 5$ for Ruddlesden–Popper $(BA)_2(MA)_{n-1}Pb_nI_{3n+1}$ perovskite are investigated in this work. For the single junction 2D PSCs with an opaque Ag electrode, the calculated *J*–*V* curves and photovoltaic parameters are shown in Figs. 2(a) and 2(b). It can be observed that the J_{sc} increases with n value increasing, but the V_{oc} shows the opposite trend, and there is no significant change for the *FF*, the resulting PCE continuously increases when the value of n is lower than 4 and begins to degrade when the value of n is set to 5. Thus the quasi-2D PSCs with $n = 3$, 4, and 5 (PCE = 15.34%, 17.63%, and 17.53%) can achieve higher PCE and more balance between photovoltaic performance and stability, which is consistent with the experimental result.[47] For the lower n of 1 and 2, the wider bandgaps (2.14 eV and 2.41 eV) limit the J_{sc} and PCE, although the corresponding PSCs have larger V_{oc} and better stability. However, owing to the low absorption coefficients and poor carrier transport caused by the strong quantum confinement effect, the 2D perovskite with $n = 1$, 2 cannot be preferred for photovoltaic applications.

For the 4T-tandem device of 2D perovskite top cell and Si bottom cell, the efficient segmented spectral absorption between sub-cells is a key to optimizing the overall PCE of tandem devices. Here, the semitransparent 2D PSCs ($n = 1$, 2, 3, 4, 5) with an ITO rear electrode are stacked with the Si heterojunction cells. Figure 3 displays the calculated photon absorption and *J*–*V* curves of 4T perovskite/Si tandem devices. It can be seen that the semitransparent 2D PSCs mainly absorb the incident photons at short wavelength and the Si bottom cell harvests the long wavelength photons filtered by the top cell, and the light absorption of sub-cells can be tuned by the n value of 2D perovskite. When it comes to the photoelectric conversion capacity, the semitransparent 2D PSC shows a lower PCE than that of opaque 2D PSC (Fig. 2), which is due to the transmission loss caused by the ITO electrode. Even so,

their PCEs increase with the n value increasing from 10.40% ($n = 1$) to 17.39% ($n = 4$). However, comparing with the reference Si cell with a PCE of 24.4% and J_{sc} of 36.83 mA/cm^2, the J_{sc} and PCE of the filtered Si bottom cell rapidly degrade to 25.88 mA/cm^2(by 36.9%) and 15.39% (by 29.7%) when n equals 1, and further decreases to 18.59 A/cm^2 and 11.29% with the value of n increasing from 1 to 5. The corresponding overall PCEs of 4T tandem devices are 25.79% ($n = 1$), 28.29% ($n = 2$), 28.51% ($n = 3$), 28.83% ($n = 4$), and 28.67% ($n = 5$), respectively. Obviously, the tandem devices with top 2D PSCs ($n = 3$, 4, 5) have acquired a PCE close to the theoretical efficiency limit of Si cells.

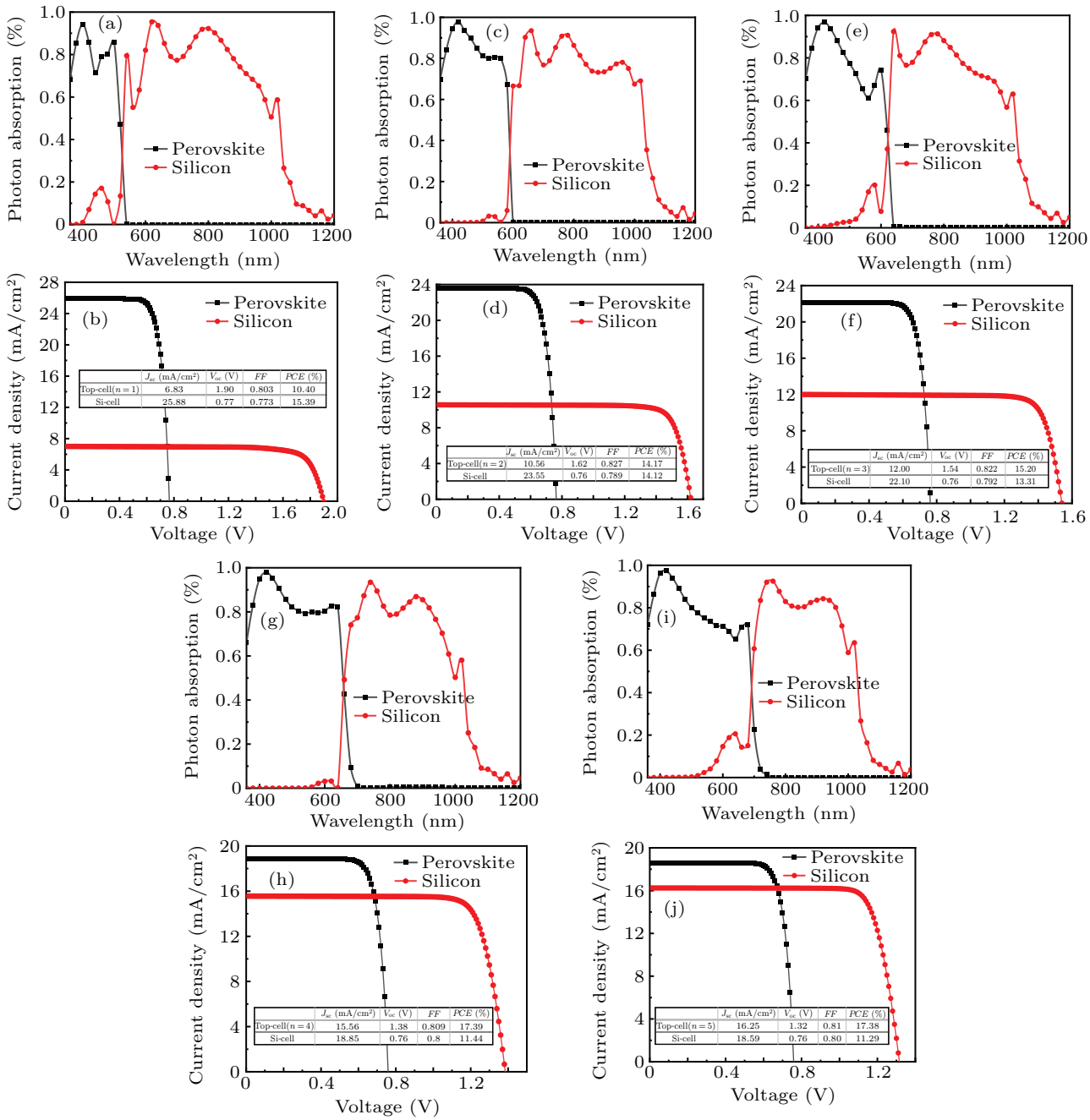


Fig. 3. Calculated absorption spectra and J–V curves of quasi-2D perovskite/Si tandem solar cells with different n values.

In order to further improve the PCE of perovskite/silicon tandem solar cells, reducing the refection loss at the top-cell/air interface may be an efficient optical strategy, and typical various thickness anti-reflection layers of LiF are used to cap the top 2D PSCs. Compared with the highest PCE of 2D perovskite ($n = 4$)/Si tandem devices, the overall PCE as a function of LiF thickness is shown in Fig. 4(a), and it can be observed that the optimal thickness of LiF anti-reflection layer is about 90 nm, corresponding to an improvement of 30.58% in PCE. Also in Fig. 4(b), for the 2D top PSCs with 90nm-thick LiF and different values of n, all the PCEs of tandem devices are enhanced noticeably and exceed 30% when the value of n equals 3, 4, and 5. The detailed J–V curves of sub-cells can be found in Fig. S1 in the supporting informa-

tion. Therefore, only by adding an anti-reflection layer, the PCE of quasi-2D perovskite/Si tandem device can surpass the theoretical efficiency limit of Si cells, which is also comparable to those of both 4T 3D-perovskite (hybrid or inorganic)/Si tandem devices and the 2T perovskite/Si tandem cells. At the same time, the quasi-2D perovskites provide a selection of tandem structure with longer operation stability.

The optimized photovoltaic performance of quasi-2D perovskite ($n = 4$)/Si tandem device is further discussed in Fig. 5. The top PSC shows a PCE of 19.05% with J_{sc} = 17.09 mA/cm^2, $V_{oc} = 1.39$ V, and $FF = 0.8$; the bottom Si cell realizes a PCE of 11.53% with J_{sc} = 19.00 mA/cm^2, $V_{oc} = 0.76$ V, and $FF = 0.8$; and the tandem device achieve a total PCE as high as 30.58%. It is apparent that the substantially enhanced J_{sc} by 9.8% is responsible for the champion PCE, which is confirmed by the obvious increase of photoabsorption in the wavelength from 500 nm to 700 nm as shown in Fig. 5(b). The relatively large intensity of optical electric field at 540 nm and 640 nm in Fig. 5(d) accord well with the above results. Simultaneously, the introduction of LiF layer triggers off an oscillation behavior of absorption in the Si bottom cell (Fig. 5(c)), but still be helpful for the Si bottom cell as J_{sc} (0.15 mA/cm^2) increases slightly. In addition, the PCE and J_{sc} loss of bottom Si cell are 52.7% and 48.4% in comparison with those of the reference Si cell, respectively, which, however, are still lower than the 63.7% and 63.8% of the most efficient 3D-perovskite/Si tandem cells.[14] In other words, the employing of quasi-2D top PSC in 4T tandem devices can make the total PCE exceed 30% and reduce the power loss of Si bottom cells.

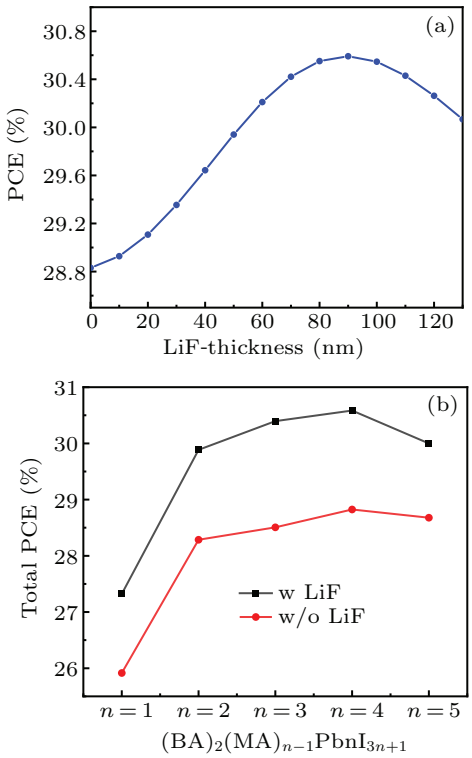


Fig. 4. Overall PCEs of tandem solar cells (a) with various thickness LiF anti-reflection layers and (b) with/without (w/o) a 90-nm LiF layer at different values of n.

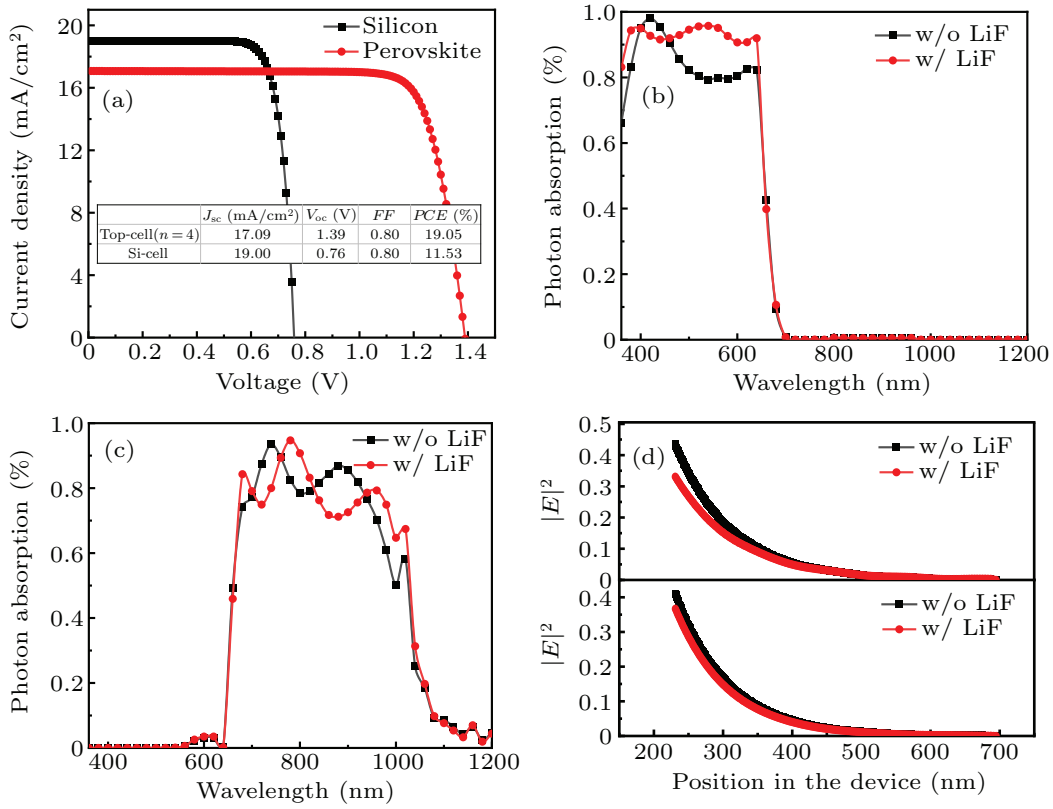


Fig. 5. (a) Calculated J–V curves of optimal quasi-2D perovskite ($n = 4$)/Si tandem solar cells with a 90-nm-thick LiF antireflection layer, absorption curves of (b) top cell, and (c) bottom cell, and (d) optical electric field distributions of top cell at wavelengths of 550 nm and 640 nm with/without (w/o) antireflection layer.

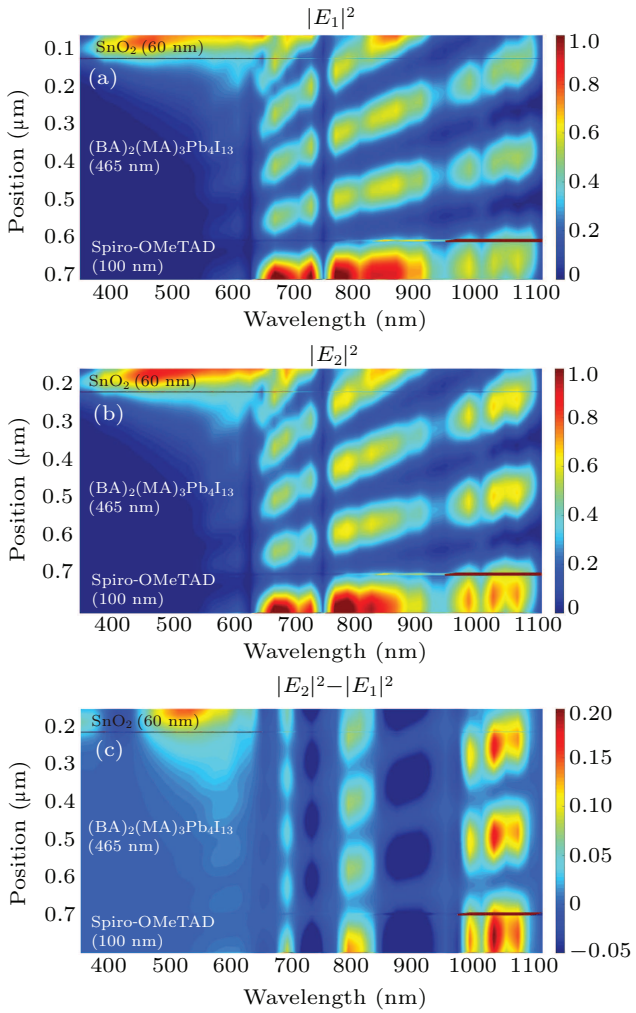


Fig. 6. Optical electric field distributions of tandem cells (a) with and (b) without LiF antireflection layer. (c) Difference between electric field distributions in panels (a) and (b) after adding LiF antireflection layer.

Furthermore, the 3D images of optical electric field distributions as a function of wavelength and position in top quasi-2D ($n = 4$) PSCs are shown in Fig. 6 to understand the optical mechanisms. Here, E_1 and E_2 represent the optical electric field in 2D PSCs without and with an LiF antireflection layer. In Figs. 6(a) and 6(b), most of the photons at short wavelengths in a range of 300 nm–700 nm are absorbed by the top 2D perovskites; while the electric field distributions at the long wavelength ranging from 700 nm to 1100 nm determine the photon energy that can be harvested by the Si bottom cell and the obvious oscillation of electric field distributions accords with the behavior of photoabsorption in Fig. 5(c). At the same time, the overall intensity of optical electric field in quasi-2D PSCs is slightly enhanced after utilizing the LiF anti-reflection layer, which can be clearly distinguished by the difference in electric field intensity displayed in Fig. 6(c). Here, the negative intensity near 750 nm and 900 nm are consistent with the interference minimum of absorption in Fig. 5(c), and the positive intensities at all other wavelengths prove the optical modulation effect of LiF anti-reflection layer. On the other hand, the 4T quasi-2D ($n = 5$) perovskite/Si tandem devices also obtain a total PCE of 30% (see Fig. S5); what is interesting is the current density of top and bottom cells (17.79 mA/cm^2 and 18.17 mA/cm^2) are very close to each other, thus the natural current matching makes it possible to construct a 2T-tandem devices of quasi-2D ($n = 5$) PSCs and Si bottom cells. Therefore, this work may open the door to the design and fabrication of quasi-2D perovskite/Si tandem devices with both 4T and 2T structures. Of course, the more efficient reflective layers (double or triple), organic-spacer-cation design, composition and device engineering can be used to improve the performance of quasi-2D top PSCs, and the experimental investigation will go further in future.

4. Conclusions

Semitransparent quasi-2D RP PSCs are introduced for the first time to construct 4T tandem devices with the Si-heterojunction bottom cells. By establishing the Atlas device model and performing systemic simulations from optical and electrical aspects, a PCE over 30% is achieved for quasi-2D $(BA)_2(MA)_{n-1}Pb_nI_{3n+1}$)/Si tandem cells with three values of n (3, 4, and 5) and the LiF anti-reflection layer at the air/top cell interfaces. When n equals 4, corresponding to a perovskite bandgap of 1.9 eV, the optimized top quasi-2D PSC and bottom Si cell show a PCE of 19.05% and 11.53%, respectively, and the total PCE of the tandem device reaches 30.58%, which exceeds the theoretical efficiency limit of Si based solar cells. More importantly, compared with the traditional 3D PSC, the quasi-2D PSC possesses a comparable PCE and can obviously improve air, phase, and thermal stability. Therefore, the 4T quasi-2D perovskite/Si device provides a more cost-effective tandem strategy and long-term stability solution. This work is instructive for designing and fabricating the perovskite/Si tandem solar cells.

Acknowledgements

Project supported by the National Natural Science Foundation of China (Grant Nos. 62004151, 62274126, 62274126, 61874083, and 61804113) and the China Postdoctoral Science Foundation (Grant No. 2020T130490).

References

[1] Chapin D M, Fuller C S and Pearson G L 1954 *J. Appl. Phys.* **25** 676
[2] Yoshikawa K, Kawasaki H, Yoshida W, Irie T, Konishi K, Nakano K, Uto T, Adachi D, Kanematsu M, Uzu H and Yamamoto K 2017 *Nat. Energy* **2** 1
[3] Richter A, Hermle M and Glunz S W 2013 *IEEE J. Photovolt.* **3** 1184
[4] Li C, Yang R and Tian H 2018 *Physics* **47** 367
[5] Beiley Z and McGehee M 2012 *Energy Environ. Sci.* **5** 9173
[6] Kojima A, Teshima K, Shirai Y and Miyasaka T 2009 *J. Am. Chem. Soc.* **131** 6050
[7] NREL https://www.nrel.gov/pv/assets/pdfs/best-research-cell-efficiencies-rev220126.pdf
[8] Wang T, Xiao G, Sun R, Luo L and Yi M 2022 *Chin. Phys. B* **31** 018801
[9] Zhang Z, Xu L and Qi J 2021 *Chin. Phys. B* **30** 038801

[10] Long C, Wang N, Huang Ke, Li H, Liu B and Yang J 2020 *Chin. Phys. B* **29** 048801
[11] Hu Y, Song L, Chen Y and Huang W 2019 *Sol. RRL* **3** 1900080
[12] Bailie C and McGehee M 2015 *MRS Bull.* **40** 681
[13] Lal N, White T P and Catchpole K 2014 *IEEE J. Photovolt.* **4** 1380
[14] Yang D, Zhang X, Hou Y, Wang K, Ye T, Yoon J, Wu C, Sanghadasa M, Liu (Frank) S and Priya S 2021 *Nano Energy* **84** 105934
[15] Choi H and Kim H 2020 *Materials* **13** 3868
[16] Liu C, Li W, Chen J, Fan J, Mai Y and Schroppcd R 2017 *Nano Energy* **41** 75
[17] Yuan H, Zhao Y, Duan J, Wang Y, Yang X and Tang Q 2018 *J. Mater. Chem. A* **6** 24324
[18] Duan J, Zhao Y, Yang X, Wang Y, He B and Tang Q 2018 *Adv. Energy Mater.* **8** 1802346
[19] Tsai H, Nie W, Blancon J, Stoumpos C, Asadpour R, Harutyunyan B, Neukirch A, Verduzco R, Crochet J, Tretiak S, Pedesseau L, Even J, Alam M, Gupta G, Lou J, Ajayan P, Bedzyk M, Kanatzidis M and Mohite A 2016 *Nature* **536** 312
[20] Hu J, Oswald I, Stuard S, Nahid M, Zhou N, Williams O, Guo Z, Yan L, Hu H, Chen Z, Xiao X, Lin Y, Yang Z, Huang J, Moran A, Ade H, Neilson J and You W 2019 *Nat. Commun.* **10** 1
[21] Fu W, Chen H and Jen A 2021 *Mater. Today Nano* **14** 100117
[22] Lee J, Dai Z, Han T, Choi C, Chang S, Lee S, Marco N, Zhao H, Sun P, Huang Y and Yang Y 2018 *Nat. Commun.* **9** 1
[23] Lai X, Li W, Gu X, Chen H, Zhang Y, Li G, Zhang R, Fan D, He F, Zheng N, Yu J, Chen R, KoKyaw A and Sun X 2022 *Chem. Eng. J.* **427** 130949
[24] Ahmad S, Fu P, Yu S, Yang Q, Liu X, Wang X, Wang X, Guo X and Li C 2019 *Joule* **3** 794
[25] Shao M, Bie T, Yang L, Gao Y, Jin X, He F, Zheng N, Yu Y and Zhang X 2022 *Adv. Mater.* **34** 2107211
[26] Zhang Y and Park N G 2022 *ACS Energy Lett.* **7** 757
[27] Wu G, Yang T, Li X, Ahamd N, Zhang X, Yue S, Zhou J, Li Y, Wang H, Shi X, Liu S, Zhao K, Zhou H and Zhang Y 2021 *Matter* **4** 582
[28] Song B, Hou J, Wang H, Sidhik S, Miao J, Gu H, Zhang H, Liu S, Fakhraai Z, Even J, Blancon J, Mohite A and Jariwala D 2021 *ACS Mater. Lett.* **3** 148
[29] Manzoor S, Häusele J, Bush K, Palmstrom A, Carpenter J, Yu Z, Bent S, Mcgehee M and Holman 2018 *Opt. Express* **26** 27441
[30] Filipič M, Löper P, Niesen B, Wolf S D, Krč J, Ballif C and Topič M 2015 *Opt. Express* **23** A263
[31] Jiang Y, Pillai S and Green M 2016 *Sci. Rep.* **6** 1
[32] Li H 1976 *J. Phys. Chem. Ref. Data* **5** 329
[33] Chen Y, Meng Q, Zhang L, Han C, Gao H, Zhang Y and Yan H 2019 *J. Energy Chem.* **35** 144
[34] Ho-Baillie A, Zhang M, Lau C, Ma F and Huang S 2019 *Joule* **3** 938
[35] He T, Li S, Jiang Y, Qin C, Cui M, Qiao L, Xu H, Yang J, Long R, Wang H and Yuan M 2020 *Nat. Commun.* **11** 1
[36] Guo Y, Wang J, Huang R and Wang G 2002 *J. Inorg. Mater.* **17** 131
[37] Oppong-Antwi L, Huang S, Li Q, Chi D, Meng X and He L 2017 *Sol. Energy* **141** 222
[38] Zhou Q, Duan J, Du J, Guo Q, Zhang Q, Yang X, Duan Y and Tang Q 2021 *Adv. Sci.* **8** 2101418
[39] Meng W, Hou Y, Karl A, Gu E, Tang X, Osvet A, Zhang K, Zhao Y, Du X, Cerrillo J, Li N and Brabec C 2019 *ACS Energy Lett.* **5** 271
[40] Liu C, Xi H, Yan H, Yang H, Chen D, Dong H, Zhu W, Zhang J, Zhang C and Hao Y 2021 *Semicond. Sci. Technol.* **36** 065019
[41] Duong T, Pham H and Kho T 2020 *Adv. Energy Mater.* **10** 1903553
[42] Zhao P, Yue M, Lei C, Lin Z, Su J, Chen D, Zhang C, Zhang J, Chang J and Hao Y 2018 *IEEE J. Photovolt.* **8** 1685
[43] He F, Fei W, Wang Y, Liu C, Guo Q, Lan W, Fan G, Lu G, Chen D, Zhu W, Xi H and Zhang C 2021 *IEEE Photon. J.* **13** 8400108
[44] Liu C, Zhang C, Pang S, Dong H, Zhang Z, Chen D, Zhu W, Zhang J and Hao Y 2020 *IEEE Photon. J.* **12** 18400312
[45] Quan L, Yuan M, Comin R, Voznyy O, Beauregard E, Hoogland S, Buin A, Kirmani A, Zhao K, Amassian A, Kim Dong and Sargen E 2016 *J. Am. Chem. Soc.* **138** 2649
[46] Passarelli J, Fairfield D, Sather N, Hendricks M, Sai H, Stern C and Stupp S 2018 *J. Am. Chem. Soc.* **140** 7313
[47] Liang C, Gu H, Xia Y, *et al.* 2021 *Nat. Energy* **6** 38